

# Pseudo energy wells in active systems

R. Sheshka,<sup>1</sup> P. Recho,<sup>2,3</sup> and L. Truskinovsky<sup>4,\*</sup>

<sup>1</sup>*LITEN, CEA-Grenoble, 17 rue des Martyrs, 38054 Grenoble, France*

<sup>2</sup>*Physico-Chimie Curie UMR 168, Institut Curie,*

*5 Rue Pierre et Marie Curie, 75005 Paris, France*

<sup>3</sup>*Mathematical Institute, University of Oxford, Oxford OX26GG, United Kingdom*

<sup>4</sup>*LMS, CNRS-UMR 7649, École Polytechnique, 91128 Palaiseau, France*

(Dated: September 10, 2018)

Active stabilization in systems with zero or negative stiffness is an essential element of a wide variety of biological processes. We study a prototypical example of this phenomenon at a micro-scale and show how active rigidity, interpreted as a formation of a pseudo-well in the effective energy landscape, can be generated in an overdamped ratchet-type stochastic system. We link the transition from negative to positive rigidity with correlations in the noise and show that subtle differences in out-of-equilibrium driving may compromise the emergence of a pseudo-well.

PACS numbers: 87.16.Nn, 87.19.Ff, 87.16.A-,05.40.Jc

Keywords: active matter, molecular motors, stochastic resonance, active rigidity

The response of a living system to mechanical loading depends not only on the properties of the constituents and their connectivity, but also on the presence of non-thermal endogenous driving [1]. Thus, molecular motors can either stiffen the cytoskeleton through actively generated pre-stress [2] or fluidize it by facilitating remodeling [3]. Powered by ATP hydrolysis, living systems can also operate in mechanical regimes with negative passive stiffness as in the case of hair cells [4, 5] and muscle half-sarcomeres [6, 7]. In those cases metabolic resources are used to modify the mechanical susceptibility of the system and stabilize the apparently unstable states [8–10].

At the structural level, *active rigidity* may be the outcome of tensegrity tightening [11], connectivity change [12], steric interactions [13], or the prestress exploiting strong nonlinearity of the passive response [14, 15]. ATP induced stiffening can even take place at the level of individual structural elements as in the case of the Frank-Starling effect in cardiac muscles that cannot be explained by a simple filament overlap change [16].

In this Letter we show that active rigidity can also emerge at the micro-scale level through resonant non-thermal excitation of molecular degrees of freedom as in the case of an inverted pendulum [17]. Following this inertial prototype, we construct an example of a mechanically unstable overdamped system where stabilization and creation of a new pseudo-well in the effective energy landscape can be induced by a colored noise. The proposed mechanism of rigidity generation requires a finite distance from equilibrium and is therefore different from the more conventional entropic stabilization [18]. The possibility of actively tunable rigidity opens interesting prospects not only in biomechanics [19] but also in engineering design incorporating negative stiffness [20] or aiming at synthetic materials stabilized dynamically [21, 22].

We illustrate our idea on a simple bi-stable mechanical

system described by a single collective variable: the negative stiffness is viewed as a result of coarse-graining in a microscopic system with domineering long range interactions [23]. We assume that this ‘snap-spring’ is exposed to both thermal and correlated noises and acts against a linear spring which qualifies it as a molecular motor operating in stall conditions [24]. Instead of the conventional focus on active force, we study in this Letter a possibility of generating by this motor active susceptibility.

The advantage of our analytically transparent setting is that we can distinguish the separate effects of thermal (scaled with temperature  $D$ ) and non-thermal (scaled with affinity  $A$ ) components of the noise on the effective energy landscape. We construct a non-equilibrium phase diagram in the space of parameters  $(D, A)$  showing that bifurcations connecting different *dynamic phases* may be either sub-critical, indicating a first order phase transition, or super-critical, indicating a second order phase transition, with the overall behavior controlled by a tricritical point. Some features of the observed dynamic transitions are reminiscent of the behavior of the Ising model in periodic magnetic field [25] and the behavior of folded proteins subjected to periodic forces [26]. We show however, that our system is highly sensitive to the stochastic nature of the nonequilibrium reservoir. Thus, in case of a periodic or dichotomous (DC) rocking force, a pseudo energy well exists in an extended domain of the parameter space, while it completely disappears if the noise is of Ornshtein-Uhlenbeck (OU) type.

*Model.* Consider the non-dimensional Langevin equation  $\dot{x} = -\partial_x E + \sqrt{2D}\xi(t)$ , where  $\xi(t)$  is a standard delta correlated noise with zero average,  $D$  is a measure of temperature and  $E(x, z, t) = V(x) + k(x - z)^2/2 - xf(t)$  is a time dependent potential. We assume that  $V(x) = (|x| - 1/2)^2/2$  is a bi-stable potential describing the conformational change and  $z$  is a control parameter coupled through a spring of stiffness  $k$  with the internal variable

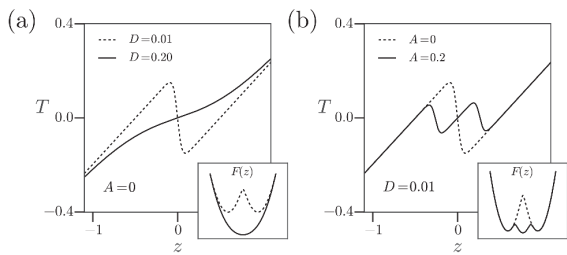


FIG. 1. Force-elongation curves in the case of periodic driving (adiabatic limit). The equilibrium system ( $A = 0$ ) is shown in (a) and out-of-equilibrium system ( $A \neq 0$ ) - in (b). Here  $k = 0.6$ .

$x$ . The energy is supplied to the system by a rocking force  $f(t)$  characterized by an amplitude  $A$  and a time scale  $\tau$ . The presence of a thermal noise in this mean field description suggests that the system has a finite size [27]. The external force required to maintain the system in the steady regime is  $T(z) = k[z - \langle x \rangle]$ , where  $\langle x \rangle = \lim_{t \rightarrow \infty} (1/t) \int_0^t \int_{-\infty}^{\infty} xp(x, t) dx dt$  is the double averaging over ensemble and time and  $p(x, t)$  is the corresponding probability distribution.

The main object of our study is the *effective potential*  $F(z) = \int^z T(s) ds$ . While  $z$  has been introduced as a constant parameter, it can be also viewed as a mesoscopic variable satisfying  $\nu \dot{z} = -\partial_z E + f_{ext} + \sqrt{2\nu D} \xi(t)$  where the frictional timescale  $\nu/k \gg \tau$  and  $f_{ext}$  is a slowly varying external force. As we show in [28] the dynamics of the ensemble and time averaged  $z$  that we denote by  $Z$  is governed by  $\nu \dot{Z} = -\partial_Z F + \overline{f_{ext}}$ . In the case of skeletal muscles, if  $x$  characterizes the state of a generic cross bridge,  $Z$  would be a measure of strain at the level of the whole half-sarcomere [28]. Even in the absence of an explicit mesoscopic variables, the concept of an effective potential is useful for the study of the slow component of the motion [29].

*Periodic driving.* Suppose first that the driving is square shaped  $f(t) = A(-1)^{n(t)}$  with  $n(t) = \lfloor 2t/\tau \rfloor$ , where brackets denote the integer part. An analytically transparent case is when the correlation time  $\tau$  is much larger than the escape time for the bi-stable potential  $V$ , e.g. [30]. For  $f(t) \equiv A$  we can find the stationary solution of the Fokker-Planck equation (with  $z = const$ )  $\partial_t p = \partial_x [p \partial_x E + D \partial_x p]$  analytically, compute  $\langle x(A) \rangle$  explicitly and then average the result over the period  $\langle \langle x \rangle \rangle = [\langle x(A) \rangle + \langle x(-A) \rangle]/2$ , see [28] for details. The typical force-elongation curves  $T(z)$  and the corresponding potentials  $F(z)$ , obtained in such adiabatic limit, are shown in Fig. 1. The equilibrium system with  $A = 0$  exhibits negative stiffness at  $z = 0$  where the effective potential  $F(z)$  has a maximum (spinodal state). As temperature increases at  $A = 0$  we observe a standard entropic stabilization of the configuration  $z = 0$ , see Fig. 1(a), which takes place as a second

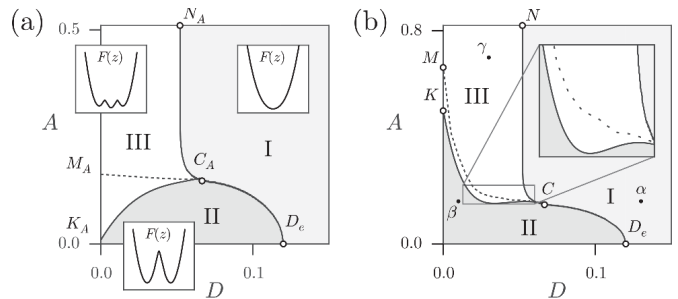


FIG. 2. Phase diagram in  $(A, D)$  plane showing phases I, II and III: (a) - adiabatic limit, (b) - numerical solution at  $\tau = 100$  (b).  $C_A$  is the tri-critical point,  $D_e$  is the point of second order phase transition in a passive system. The Maxwell line for first order phase transition is shown by dots. Here  $k = 0.6$ .

order phase transition at the equilibrium temperature  $D_e = r/[8(1+k)]$  where  $r$  is a root of a transcendental equation  $1 + \sqrt{r/\pi} e^{-1/r} / [1 + \text{erf}(1/\sqrt{r})] = r/(2k)$  [28]. As the degree of non-equilibrium, characterized by  $A$ , increases, the effective potential develops a pseudo-well with a minimum at  $z = 0$ , see Fig. 1(b), and we associate this phenomenon with the emergence of active rigidity.

The non-equilibrium steady state (dynamic) phase diagram summarizing the results obtained in adiabatic approximation is shown in Fig. 2 (a). There, the 'paramagnetic' phase I describes the regimes where the effective potential  $F(z)$  is convex, the 'ferromagnetic' phase II is a bi-stability domain where the potential  $F(z)$  has a double well structure and, finally, phase III is where the function  $F(z)$  has three *convex* branches separated by two concave (spinodal) regions. If we interpret the boundary  $C_A - D_e$  separating phases I and II as a line of (zero force) second order phase transitions and the dashed line  $C_A - M_A$  as a Maxwell line for the (zero force) first order phase transition, see [28], then  $C_A$  will be a tri-critical point. Near this point the system can be described by the non-equilibrium Landau potential  $F(z) = F_0 + rz^2 + qz^4 + pz^6$  where the coefficients  $r, q$  are the measures of passive and active excitations, respectively, while  $p > 0$  is a fixed parameter. Similar tri-critical point has been observed in the periodically driven mean field Suzuki-Kubo model of magnetism [31] which can be interpreted in our terms as a description of the  $T = 0$  behavior only.

The adiabatic approximation fails at low temperatures (small  $D$ ) where the escape time diverges and in this domain the corrected phase diagram was obtained numerically by computing the appropriate periodic solutions of the Fokker-Planck equation, see Fig. 2 (b). The high temperature part of the diagram (tri-critical point, point  $D_e$  and the vertical asymptote of the boundary separating phases I and III at large values of  $A$  are captured adequately by the adiabatic approximation. The new feature is a dip of the boundary separating Phases II and III at

some  $D < D_e$  leading to an interesting re-entrant behavior (cf. [32, 33]) which is an effect of stochastic resonance. To verify our numerics in the low temperature domain we used the Kramers approximation, to show that indeed  $A = 1/2$  at point  $K$  and  $A = 1/2 + k/4$  at point  $M$ , see [28].

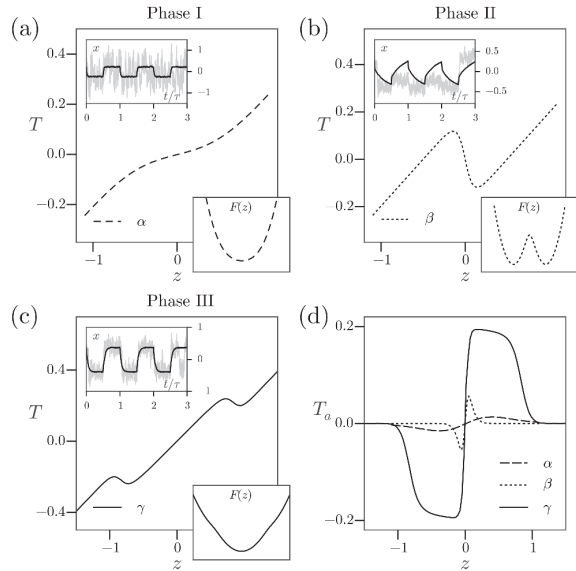


FIG. 3. (a-c) Typical tension-length relations in phases I, II and III. Points  $\alpha$ ,  $\beta$  and  $\gamma$  are the same as in Fig. 2 (b); (d) shows the active component of the force. Inserts illustrate the behavior of stochastic trajectories in each of the phases (gray lines) and their ensemble averages (black lines) at  $z \simeq 0$ . The other parameters:  $k = 0.6$ ,  $\tau = 100$ .

Force-elongation relations in different points of the  $(A, D)$  phase diagram (Fig. 2 (b)) are shown in Fig. 3 where the insets illustrate the typical stochastic trajectories. We observe that while in phase I thermal fluctuations dominate periodic driving and undermine the two wells structure of the potential, in phase III the jumps between the two energy wells are fully synchronized with the rocking force. In phase II the system shows intermediate behavior with uncorrelated jumps between the wells. We conclude that the pseudo-well in phase III has a resonant nature and remark that somewhat similar phenomena were also observed in other driven out-of-equilibrium systems [34].

In Fig. 3(d) we show the active component of the force  $T_a(z) = T(z; A) - T(z; 0)$  representative of phases I, II and III. The active contribution is significant only in phase III and the corresponding plateau can be viewed as another signature of the presence of a pseudo-well. Interestingly, our prototypical device generates active tension of both signs which can be interpreted as pulling at  $z > 0$  and pushing at  $z < 0$ . However, in the pulling regime the linear spring is stretched while in the pushing regime it is compressed. Since in biological conditions the filaments responsible for passive stiffness would buckle in

compression, e.g. [35], the pushing part of the active force-length relation is hardly realistic. On the other hand, the pulling part shows a striking resemblance to the isometric tetanus in skeletal muscles [36] that can be also driven through the bi-stable potential [37].

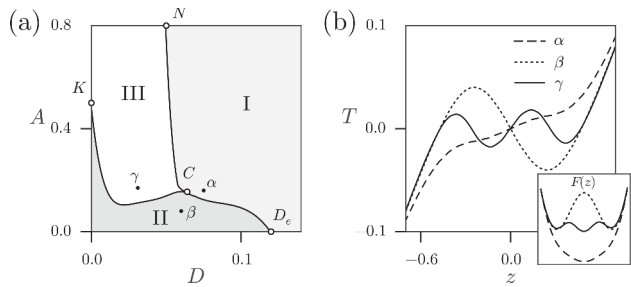


FIG. 4. (a) Phase diagram in the case of DC driving. The identification of phases I, II, III is the same as in Fig. 2 (a,b). (b) Typical tension-length relations in different phases (b). Here  $\tau = 100$  and  $k = 0.6$ .

In view of this analogy, detailed in [28], it is instructive to estimate the four non-dimensional parameters of the model by using the available data on molecular motors operating in muscle cells. We choose the time scale to be  $\tau^* = \eta/k_0 \sim 0.1$  ms where  $\eta \sim 0.38$  ms. pN/nm is the viscosity adopted in [7] and  $k_0 \sim 3$  pN/nm is the stiffness of the cross-bridge in pre and post power stroke configurations. The spatial scale is  $l^* = a \sim 10$  nm, the characteristic size of a motor power-stroke [40] and the stress scale is  $k^* = k_0$ . This leads to an energy scale  $E^* = k_0 a^2 \sim 200$  pN.nm. Then, the non-dimensional parameters can be estimated as follows. Parameter  $k = k_m/k^* \sim 0.6$ , where  $k_m$  is the stiffness of the elastic part of the myosin motor [38, 39]. Temperature is  $D = k_B \Theta / E^* \sim 0.01$  where  $k_B = 4.10$  pN.nm is the Boltzmann constant and  $\Theta \sim 300$  K the ambient temperature. For the active driving time scale, we estimate  $\tau = \tau_a / \tau^* \sim 100$  where  $\tau_a = 40$  ms is the characteristic time of ATP hydrolysis [41]. Finally we take  $A = \sqrt{\Delta\mu / E^*} \approx 0.5$  where  $\Delta\mu = 20 k_B \Theta$  is the degree of non-equilibrium of the hydrolysis reaction [41]. The obtained estimate ( $A = 0.5, D = 0.01$ ) suggests that muscle myosins, operating in stall conditions (isometric contractions), are in phase III. The proposed representation of the ATP hydrolysis (through parameter  $A$ ) explains stabilization of the power stroke mechanism in skeletal muscles in the negative stiffness regime [7] and may be also behind titin based force generating mechanism at long sarcomere lengths that does not rely on actin-myosin based cross-bridge interactions [42].

*Dichotomous driving.* To ascertain the robustness of these results we now consider a different representation of the external forcing as a dichotomous (DC) or telegraphic noise, e.g. [43, 44]. In this case  $f(t) = A(-1)^{n(t)}$ , where  $n(t)$  is a Poisson process with  $(P(n) = e^{-\lambda} \lambda^n / n!$

and rate parameter  $\lambda = 1/(2\tau)$ ; we thus have  $\langle f(t) \rangle = A \exp(-t/\tau)$  and  $\langle f(t), f(s) \rangle = A^2 \exp(-|t-s|/\tau)$ . The DC driven system is controlled by the same number of parameters as the periodically driven system, however, the problem is no longer analytically tractable. The numerical solution of the ensuing stochastic differential equation shows that the qualitative structure of the phase diagram in the  $(A, D)$  plane remains the same as in the case of periodic driving, see Fig.4. We checked our numerical results by considering an analytically tractable double limit when  $\tau \rightarrow 0$ ,  $A \rightarrow \infty$ , while  $\tilde{D} = A^2\tau$  remains finite. In this limit phase III disappears because the system can be viewed as exposed to a white noise with effective temperature  $D^* = \sqrt{D^2 + \tilde{D}^2}$ . Then there is only a second order phase transition at the expected value of the parameter  $D_e^* = r/[8(1+k)]$ . This simple limit highlights the crucial role of correlations in the noise ( $\tau \neq 0$ ). Our next example, however, shows that correlations per se are not enough.

*Ornstein-Uhlenbeck driving.* Suppose now that  $f(t)$  is a solution of a linear stochastic differential equation  $\dot{f} = -f(t)/\tau + A\sqrt{2/\tau}\xi_f(t)$ , where  $\xi_f(t)$  is a standard white noise independent of  $\xi(t)$ . Such non-equilibrium driving is known as Ornstein-Uhlenbeck (OU) noise, e.g. [44, 45], and its first ( $\langle f(t) \rangle$ ) and second ( $\langle f(s)f(t) \rangle$ ) moments are the same as in the case of DC if we assume, without loss of generality, that  $f(0) = A$ . The Fokker-Planck equation for the probability density  $p(x, f, t)$  takes the form  $\partial_t p = \partial_x(p\partial_x E + D\partial_x p) + \tau^{-1}\partial_f(fp + A^2\partial_f p)$ . By solving it numerically we obtain a phase diagram shown in Fig. 5(a). A striking feature of this diagram is that phase III is missing because, in contrast to periodic and DC case, the noise is now unbounded and the system can always escape from a neighborhood of a resonant state. The behavior of the force-elongation relations shown in Fig. 5(b) is compatible with the idea of purely entropic stabilization, in particular, the limit of thermal noise is again recovered when  $\tau \rightarrow 0$  and  $A \rightarrow \infty$ , with  $\tilde{D} = A^2\tau$  fixed.

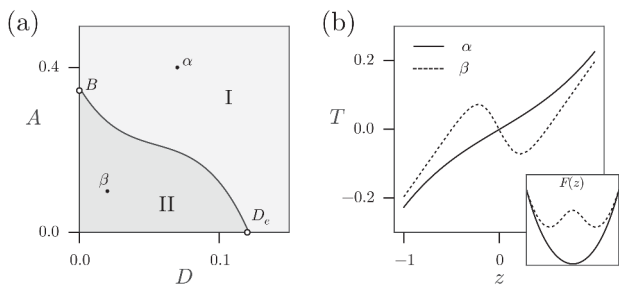


FIG. 5. (a) Phase diagram in the case of OU driving. The identification of phases I, II is the same as in Fig. 2 (a,b). (b) The typical tension-length relations in different phases. Here  $\tau = 100$  and  $k = 0.6$ .

*Zero temperature limit.* To clarify further the dif-

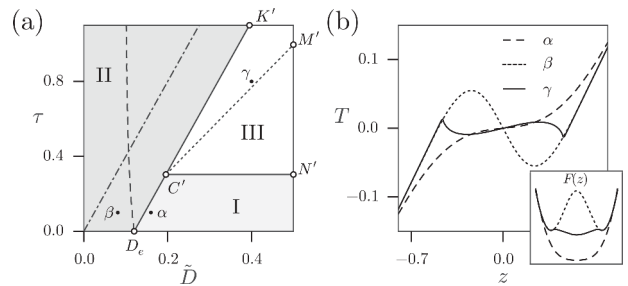


FIG. 6. (a) Phase diagram in the case of DC driving. The identification of phases I, II and III is the same as in Fig. 2 (a,b). The dash-dotted line - the boundary between phases II and III (periodic driving); the dashed line - the boundary between Phases I and II (OU driving). (b) Typical tension-length relations in the case of DC driving in different phases (b). Parameters  $k = 0.6$ ,  $D = 0$ .

ferences between our three representations of a non-equilibrium bath, we compare in all three cases the  $(\tau, \tilde{D})$  phase diagrams corresponding to the limit  $D \rightarrow 0$  where the thermal component of the noise is absent. In the DC case the solution of the limiting Fokker-Planck equation can be written explicitly [46]

$$p_{DC}(x) \sim Q(x)^{-1} \exp \left( - \int^x \frac{\partial_y \tilde{V}(y)/\tau}{A^2 - (\partial_y \tilde{V}(y))^2} dy \right).$$

where  $Q = A^2 - (\partial_x \tilde{V}(x))^2$  and  $\tilde{V} = V + k(x-z)^2/2$ . The choice of the normalization constant depends on the parameters and is detailed in [28]. The resulting phase diagram, shown in Fig. 6(a), exhibits all three phases with a tri-critical point  $C'$  located at  $\tau_{C'} = [2(k+1)]^{-1}$  and  $\tilde{D}_{C'} = D_e + [2(k+1)]^{-1}/4$ . The behavior of the force-elongation relations in different phases is illustrated in Fig. 6(b).

In the case of OU driving with  $D = 0$  an analytical approximation of the stationary probability distribution is available for small  $\tau$  only [46]

$$p_{OU}(x) \sim R(x) \exp \left( - \frac{\tilde{V}(x) + \tau(\partial_x \tilde{V}(x))^2/2}{A^2\tau} \right)$$

where  $R(x) = |1 + \tau\partial_{xx}\tilde{V}(x)|$ , see [28] for the details. The resulting phase diagram does not contain phase III and the line dividing phases I and II is shown in Fig. 6(a) (dashed line). The problem with periodic driving exhibits in the limit  $D \rightarrow 0$  only phases II and III even for rapidly oscillating external fields, see the dash-dotted line in Fig. 6(a). In this perspective, the DC driving emerges as an intricate amalgam of OU and periodic noises with none of them dominating the other.

*Conclusions.* To complement the existing microscopic models of force generation (Brownian ratchets), we proposed a conceptually similar model of rigidity generation (Brownian snap-springs). The model, invoking some

interesting parallels between condensed matter physics and biomechanics, shows that by controlling the degree of non-equilibrium in the system, one can modify the structure of the effective energy landscape. In particular, this implies that unstable or marginally stable mechanical states may be stabilized by out-of-equilibrium ATP hydrolysis reaction. Our results also suggest that the mechanical action of a non-equilibrium reservoir can be crucially sensitive to the higher moments of the stochastic noise.

The authors thank J.-F. Joanny, R. García García and M. Caruel for helpful discussions.

---

\* trusk@lms.polytechnique.fr

- [1] C. P. Broedersz and F. C. MacKintosh, *Rev. Mod. Phys.* **86**, 995 (2014).
- [2] G. H. Koenderink, Z. Dogic, F. Nakamura, P. M. Bendix, F. C. MacKintosh, J. H. Hartwig, T. P. Stossel, and D. A. Weitz, *PNAS* **106**, 15192 (2009).
- [3] J. Ranft, M. Basan, J. Elgeti, J.-F. Joanny, J. Prost, and F. Jülicher, *PNAS* **107**, 20863 (2010).
- [4] P. Martin, A. D. Mehta, and A. J. Hudspeth, *PNAS* **97**, 12026 (2000).
- [5] C. Batters, M. I. Wallace, L. M. Coluccio, and J. E. Molloy, *Phil. Trans. R. Soc. Lond. B* **359**, 1895 (2004).
- [6] A. Vilfan and T. Duke, *Biophys. J.* **85**, 818 (2003).
- [7] M. Caruel, J.-M. Allain, and L. Truskinovsky, *Phys. Rev. Lett.* **110**, 248103 (2013).
- [8] H. Schillers, M. Wälte, K. Urbanova, and H. Oberleithner, *Biophys. J.* **99**, 3639 (2010).
- [9] R. J. Hawkins and T. B. Liverpool, *Phys. Rev. Lett.* **113**, 028102 (2014).
- [10] J. Étienne, J. Fouchard, D. Mitrossilis, N. Bufi, P. Durand-Smet, and A. Asnacios, *PNAS*, 201417113 (2015).
- [11] D. E. Ingber, N. Wang, and D. Stamenović, *Rep. Prog. Phys.* **77**, 046603 (2014).
- [12] P. R. Onck, T. Koeman, T. van Dillen, and E. van der Giessen, *Phys. Rev. Lett.* **95**, 178102 (2005).
- [13] D. A. Fletcher and R. D. Mullins, *Nature* **463**, 485 (2010).
- [14] R. H. Pritchard, Y. Y. S. Huang, and E. M. Terentjev, *Soft Matter* **10**, 1864 (2014).
- [15] P. Ronceray, C. Broedersz, and M. Lenz, arXiv:1507.05873 (2015).
- [16] F. Kobirumaki-Shimozawa, T. Inoue, S. A. Shintani, K. Oyama, T. Terui, S. Minamisawa, S. Ishiwata, and N. Fukuda, *J. Physiol. Sci.* **64**, 221 (2014).
- [17] E. I. Butikov, *J. Phys. A: Math. Theor.* **44**, 295202 (2011).
- [18] L. Vočadlo, D. Alfè, M. J. Gillan, I. G. Wood, J. P. Brodholt, and G. D. Price, *Nature* **424**, 536 (2003).
- [19] G. Puglisi and L. Truskinovsky, *Phys. Rev. E* **87**, 032714 (2013).
- [20] F. Fritzen and D. M. Kochmann, *Int. J. Solids Struct.* **51**, 4101 (2014).
- [21] M. Bukov, L. D'Alessio, and A. Polkovnikov, *Adv. Phys.* **64**, 139 (2015).
- [22] P. Sarkar, A. Shit, S. Chattopadhyay, and S. K. Banik, *Chem. Phys.* **458**, 86 (2015).
- [23] M. Caruel, J. M. Allain, and L. Truskinovsky, *J. Mech. Phys. Solids* **76**, 237 (2015).
- [24] P. Reimann, *Phys. Rep.* **361**, 57 (2002).
- [25] R. Gallardo, O. Idigoras, P. Landeros, and A. Berger, *Phys. Rev. E* **86**, 051101 (2012).
- [26] C. Fogle, J. Rudnick, and D. Jasnow, arXiv:1502.00343 [cond-mat] (2015).
- [27] M. Paniconi and Y. Oono, *Phys. Rev. E* **55**, 176 (1997).
- [28] See *Supplemental Material* at [URL will be inserted by publisher].
- [29] A. A. Zaikin, J. Kurths, and L. Schimansky-Geier, *Phys. Rev. Lett.* **85**, 227 (2000); J. P. Baltanás, L. Lopez, I. I. Blechman, P. S. Landa, A. Zaikin, J. Kurths, and M. A. F. Sanjuán, *Phys. Rev. E* **67**, 066119 (2003); P. S. Landa and P. V. E. McClintock, *Phys. Rep.* **532**, 1 (2013); P. Sarkar, A. K. Maity, A. Shit, S. Chattopadhyay, J. R. Chaudhuri, and S. K. Banik, *Chem. Phys. Lett.* **602**, 4 (2014).
- [30] M. O. Magnasco, *Phys. Rev. Lett.* **71**, 1477 (1993).
- [31] T. Tomé and M. J. de Oliveira, *Phys. Rev. A* **41**, 4251 (1990).
- [32] C. Van den Broeck, J. M. R. Parrondo, and R. Toral, *Phys. Rev. Lett.* **73**, 3395 (1994).
- [33] K. R. Pilkievicz and J. D. Eaves, *Soft Matter* **10**, 7495 (2014).
- [34] L. F. Cugliandolo, D. R. Gempel, and C. A. da Silva Santos, *Phys. Rev. Lett.* **85**, 2589 (2000); M. A. Muñoz, F. d. l. Santos, and M. M. T. d. Gama, *Eur. Phys. J. B* **43**, 73 (2005); L. Berthier and J. Kurchan, *Nat. Phys.* **9**, 310 (2013).
- [35] M. Lenz, T. Thoresen, M. L. Gardel, and A. R. Dinner, *Phys. Rev. Lett.* **108**, 238107 (2012).
- [36] A. M. Gordon, A. F. Huxley, and F. J. Julian, *J. Physiol.* **184**, 170 (1966).
- [37] R. Sheshka and L. Truskinovsky, *Phys. Rev. E* **89**, 012708 (2014).
- [38] A. Lewalle, W. Steffen, O. Stevenson, Z. Ouyang, and J. Sleep, *Biophys. J.* **94**, 2160 (2008).
- [39] C. Barclay, R. Woledge, and N. Curtin, *Prog. Biophys. Mol. Bio.* **102**, 53 (2010).
- [40] M. Linari, M. Caremani, and V. Lombardi, *Proc. Biol. Sci.* **277**, 19 (2010).
- [41] J. Howard, *Mechanics of motor proteins and the cytoskeleton* (Sinauer Associates Inc.-Publishers Sunderland, Massachusetts, 2001).
- [42] G. Schappacher-Tilp, T. Leonard, G. Desch, and W. Herzog, *PloS one* **10** (2015).
- [43] A. Ichiki, Y. Tadokoro, and M. I. Dykman, *Phys. Rev. E* **85**, 031106 (2012).
- [44] K. H. Nagai, Y. Sumino, R. Montagne, I. S. Aranson, and H. Chaté, *Phys. Rev. Lett.* **114**, 168001 (2015).
- [45] R. Bartussek, in *Stochastic Dynamics*, Lecture Notes in Physics No. 484, edited by L. Schimansky-Geier and T. Pöschel (Springer Berlin Heidelberg, 1997) pp. 68–80.
- [46] P. Hänggi and P. Jung, in *Advances in Chemical Physics*, Vol. 89 (John Wiley & Sons Inc, 1995) pp. 239–326.